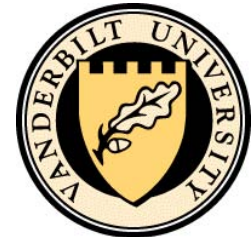


CORRELATIONS BETWEEN MULTIPARTICLE CUMULANTS AND MEAN TRANSVERSE MOMENTUM IN SMALL COLLISION SYSTEMS WITH THE CMS DETECTOR



Shengquan Tuo
(Vanderbilt University)
for the CMS Collaboration



Apr 6, 2022



U.S. DEPARTMENT OF
ENERGY

Office of
Science



INTRODUCTIONS

In heavy ion collisions:

- Final state anisotropic flow is from hydrodynamic response to initial geometry anisotropy
- Mean p_T ($[p_T]$) reflects the strength of radial flow push, which is related to the initial fireball energy density
- The correlations between v_n and $[p_T]$ probe the fluctuations of the initial density profile

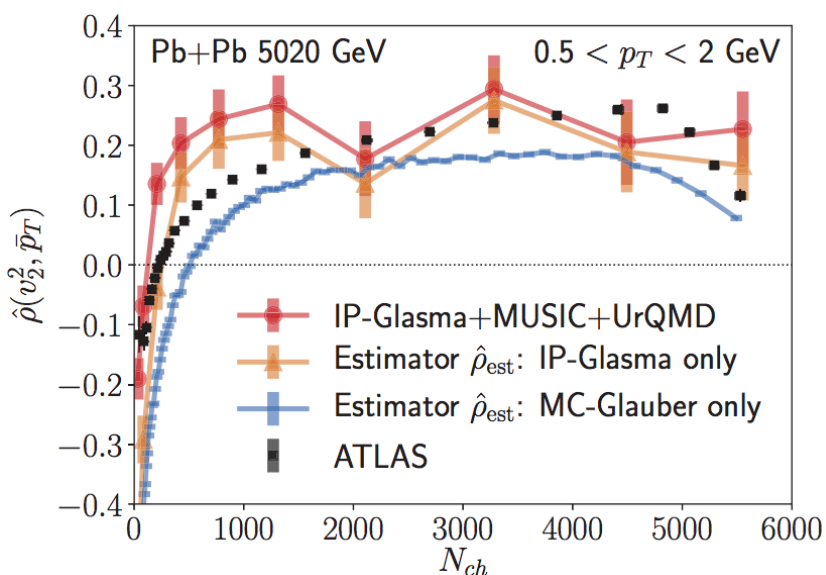
$$\rho(v_n^2, [p_T]) = \frac{\text{cov}(v_n^2, [p_T])}{\sqrt{\text{var}(v_n^2)}\sqrt{\text{var}([p_T])}}$$

INTRODUCTIONS

In heavy ion collisions:

- Final state anisotropic flow is from hydrodynamic response to initial geometry anisotropy
- Mean p_T ($[p_T]$) reflects the strength of radial flow push, which is related to the initial fireball energy density
- The correlations between v_n and $[p_T]$ probe the fluctuations of the initial density profile

$$\rho(v_n^2, [p_T]) = \frac{\text{cov}(v_n^2, [p_T])}{\sqrt{\text{var}(v_n^2)}\sqrt{\text{var}([p_T])}}$$



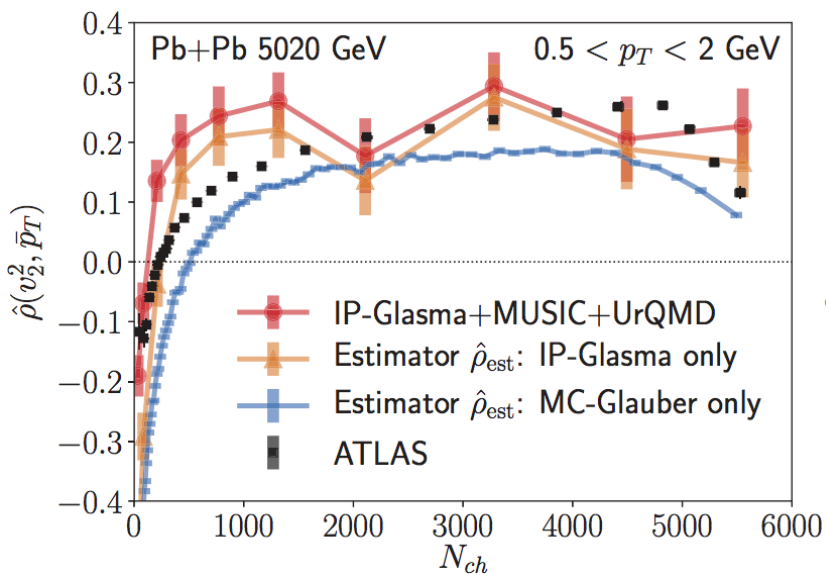
Phys. Rev. C 102, 034905 (2020)

Sensitive to the degree of sub-nucleon fluctuations

INTRODUCTIONS

In heavy ion collisions:

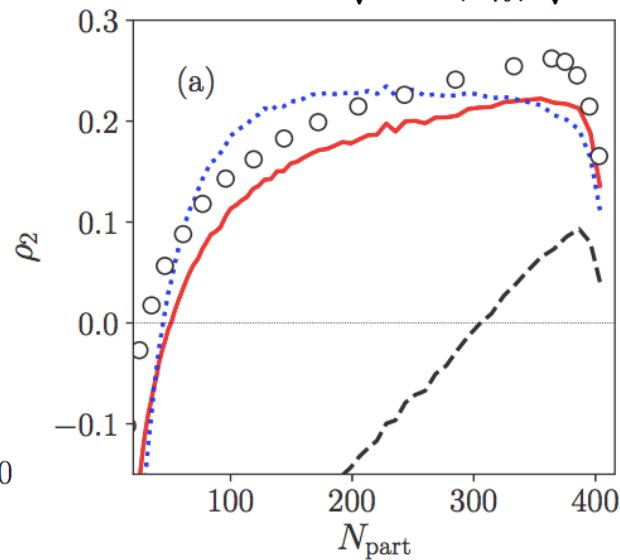
- Final state anisotropic flow is from hydrodynamic response to initial geometry anisotropy
- Mean p_T ($[p_T]$) reflects the strength of radial flow push, which is related to the initial fireball energy density
- The correlations between v_n and $[p_T]$ probe the fluctuations of the initial density profile



Phys. Rev. C 102, 034905 (2020)

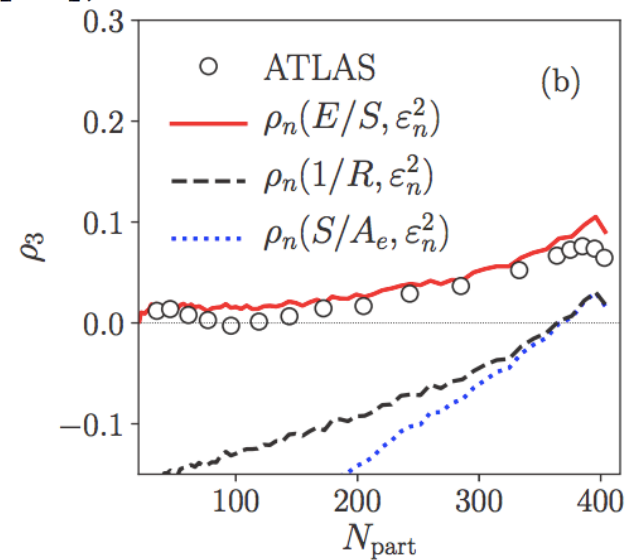
Sensitive to the degree of sub-nucleon fluctuations

$$\rho(v_n^2, [p_T]) = \frac{\text{cov}(v_n^2, [p_T])}{\sqrt{\text{var}(v_n^2)}\sqrt{\text{var}([p_T])}}$$

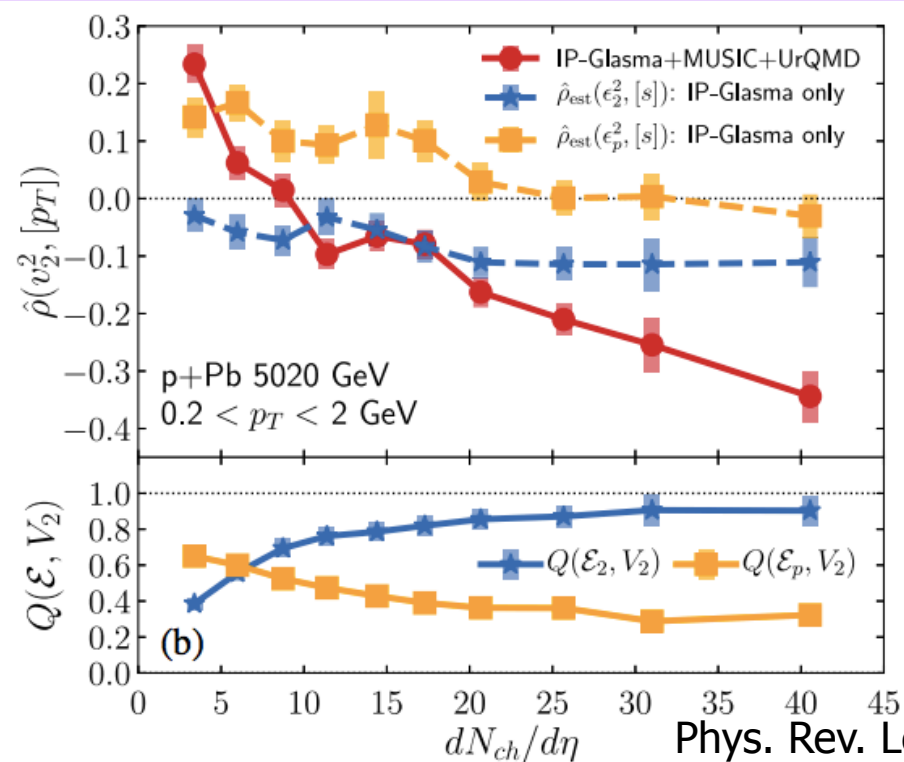


Phys. Rev. C 103, 024909 (2021)

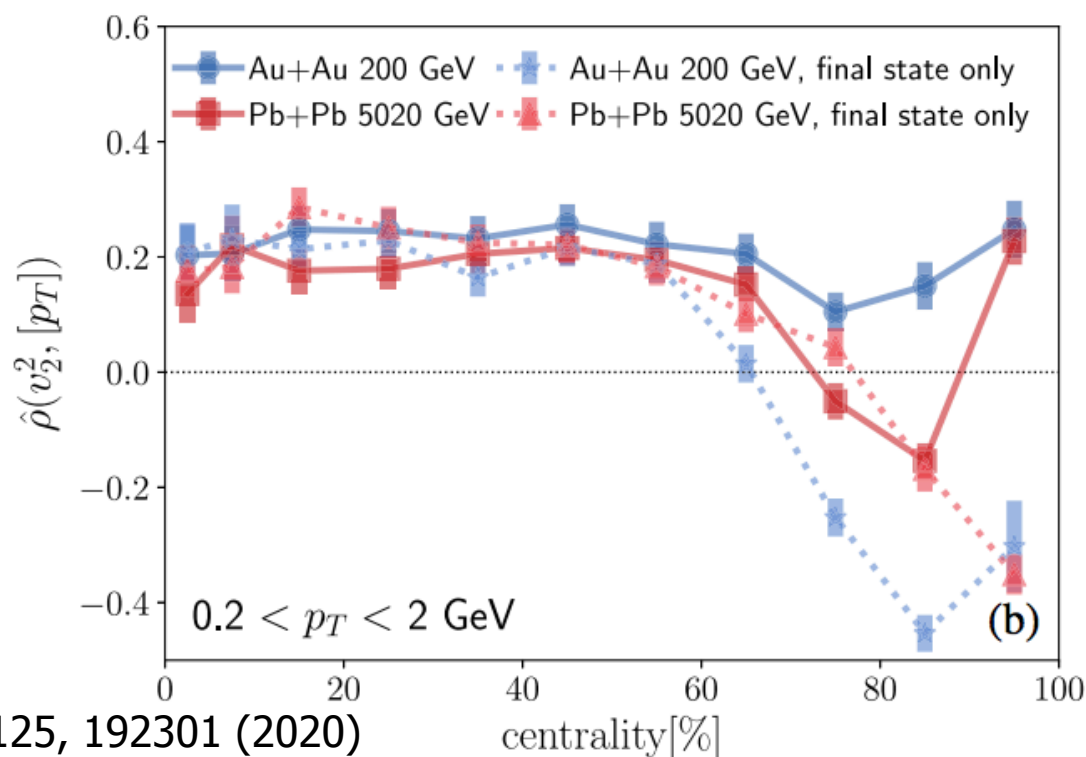
The mechanism driving the correlations can be traced back to the initial density profile



MOTIVATIONS FOR SMALL SYSTEMS (1)

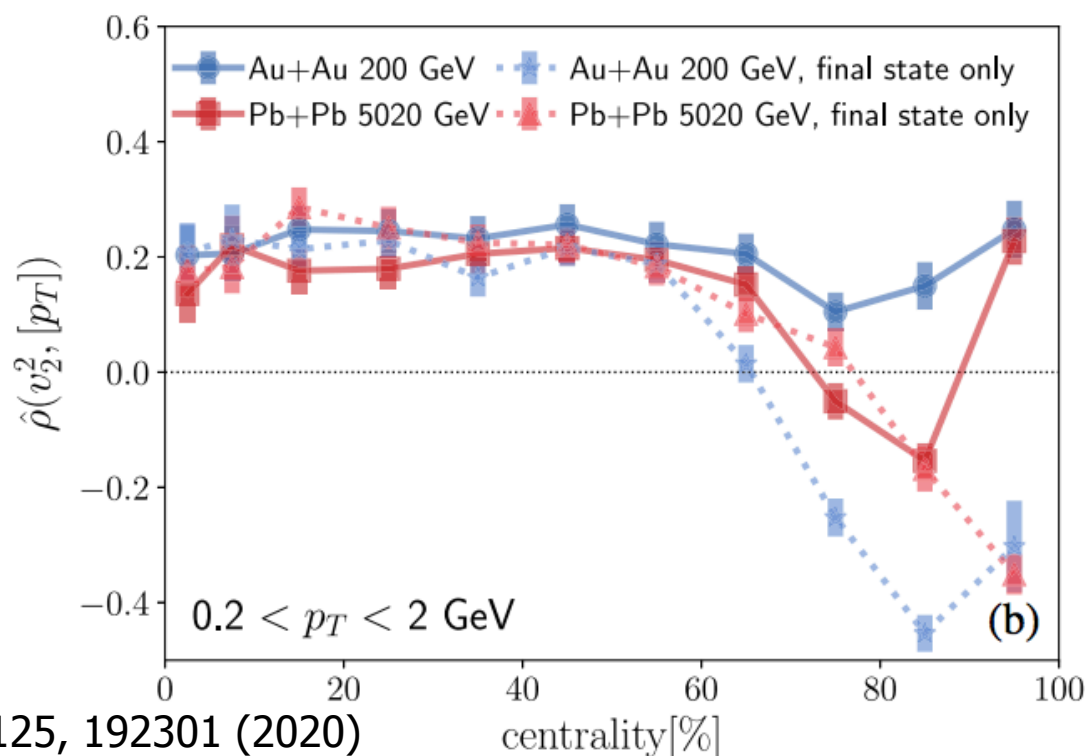
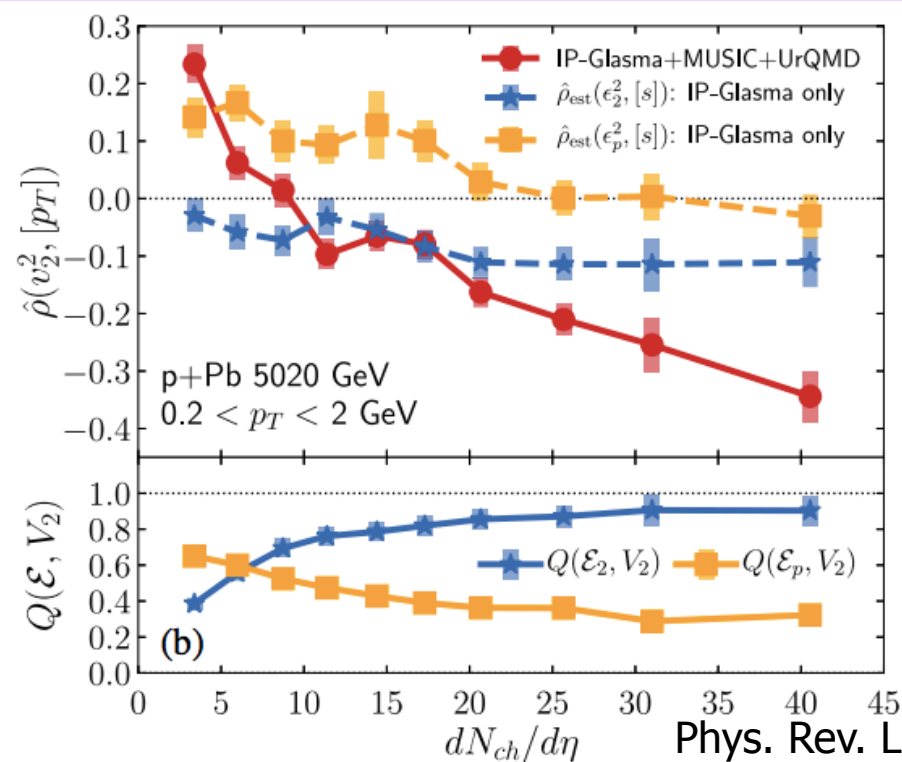


Phys. Rev. Lett. 125, 192301 (2020)

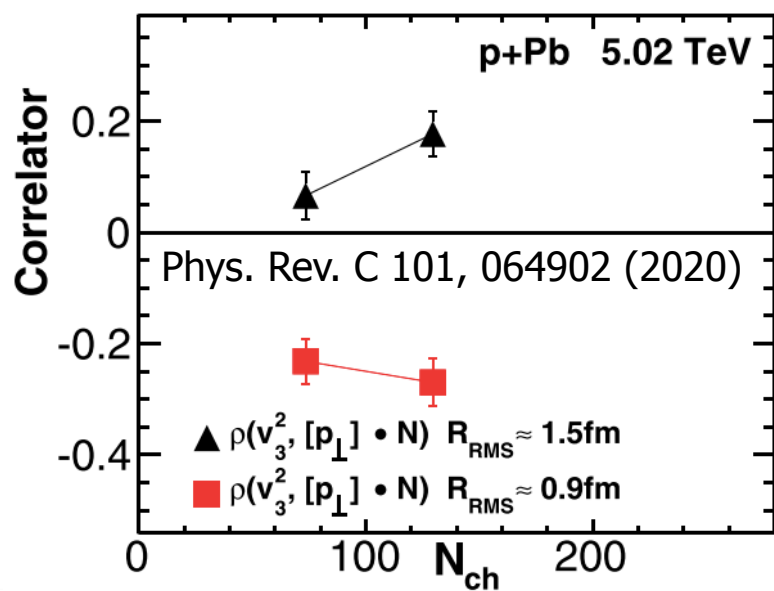


- The correlations carry information about the origin of the observed momentum anisotropy
- No sign change at low multiplicity without initial v_2 from CGC

MOTIVATIONS FOR SMALL SYSTEMS (1)

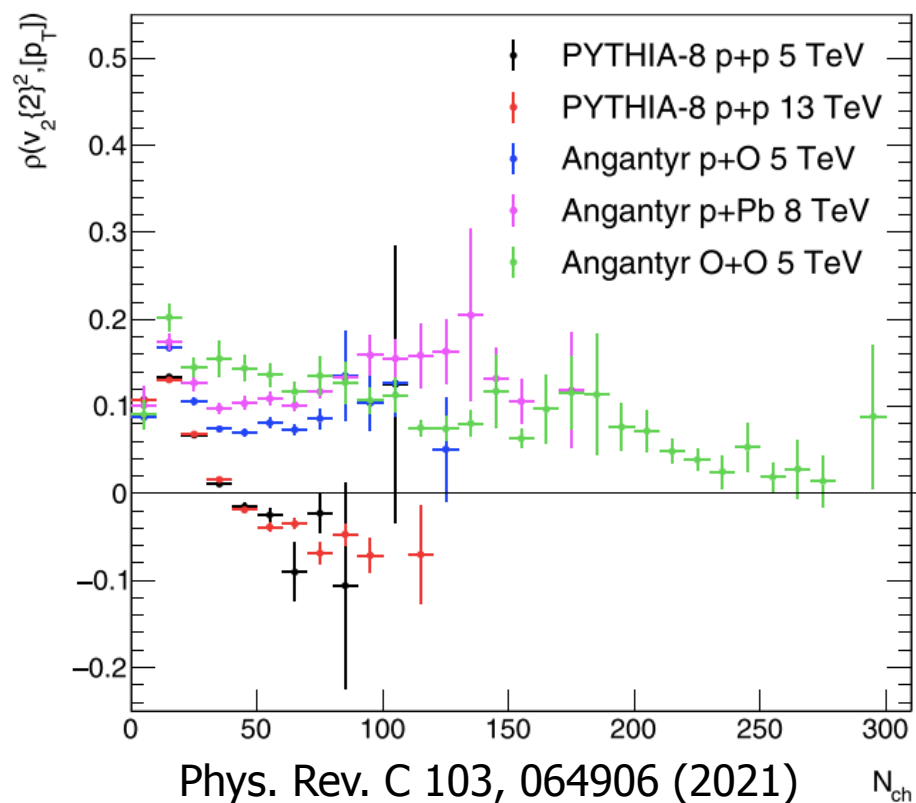
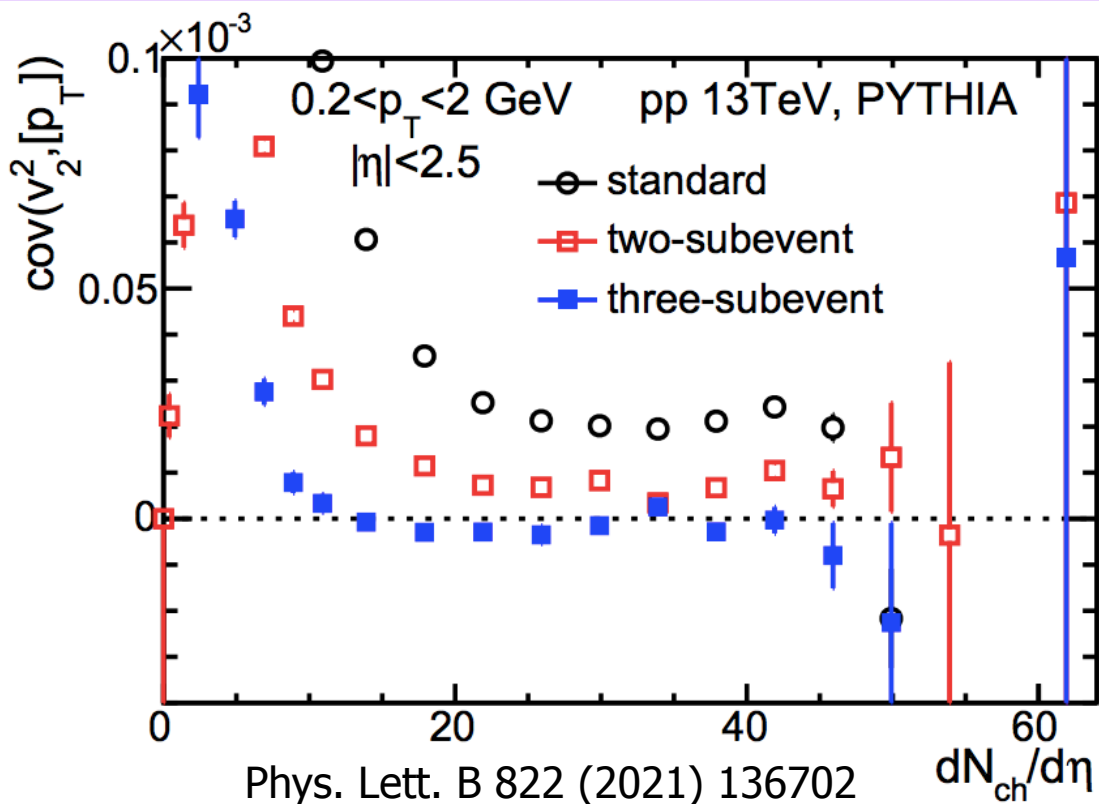


Phys. Rev. Lett. 125, 192301 (2020)



- The correlations carry information about the origin of the observed momentum anisotropy
- No sign change at low multiplicity without initial v_2 from CGC
- Sensitive to the transverse size of the initial fireball

MOTIVATIONS FOR SMALL SYSTEMS (2)

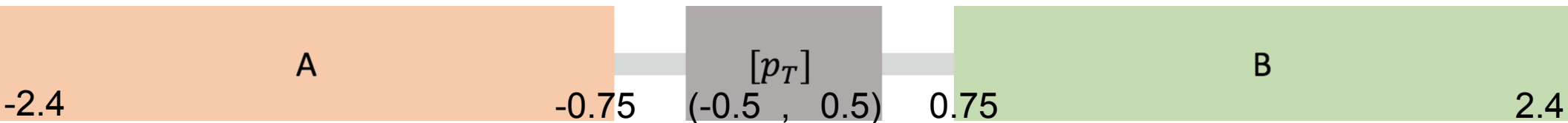


- However, the correlations from PYTHIA alone have a sign change
- Nonflow has to be carefully subtracted
- Goal of this analysis:
 - Introduce a new variable to remove more nonflow
 - Search for sign change at lowest possible multiplicity in pp/pPb/PbPb collisions

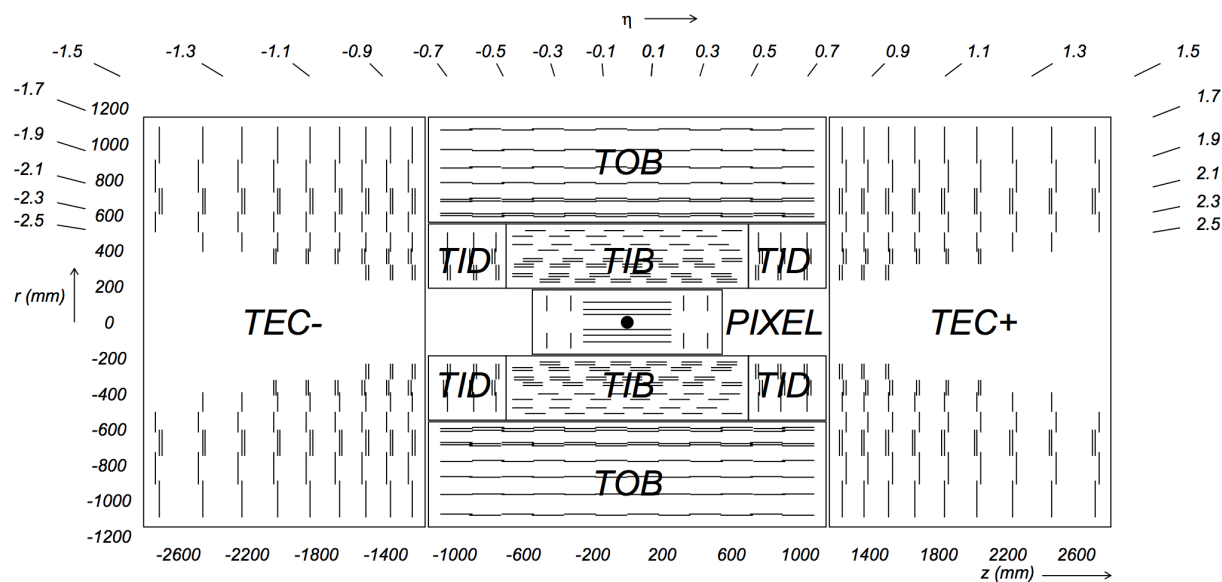
ANALYSIS METHOD (1)

$$\rho(v_2^2, [p_T]) = \frac{\text{COV}(v_2^2, [p_T])}{\sqrt{\text{Var}(v_2^2)_{dyn}} \sqrt{\text{Var}([p_T])_{dyn}}} \quad (1)$$

$\rho(c_2\{2\}, [p_T])$



Subevents A and B are used for calculation of $c_2\{2\}$; $|\eta| < 0.5$ for $[p_T]$

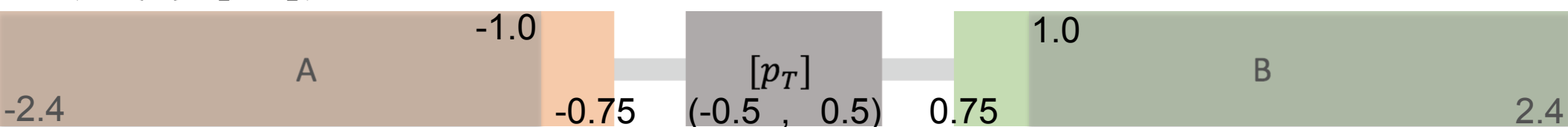


CMS Silicon Tracker, JINST 3 (2008) S08004

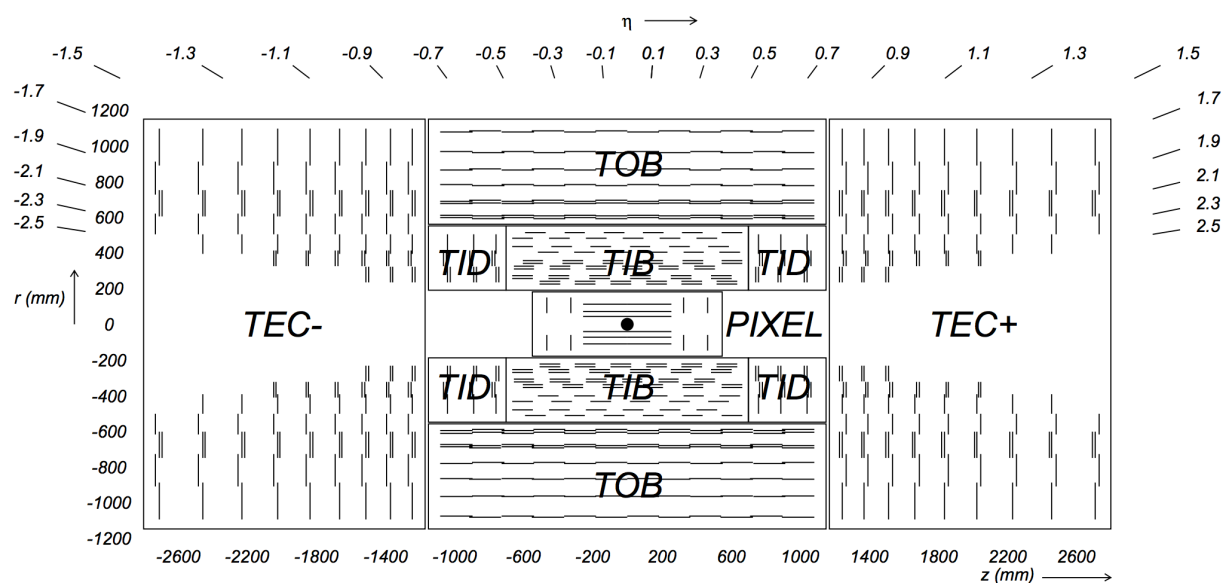
ANALYSIS METHOD (1)

$$\rho(v_2^2, [p_T]) = \frac{\text{COV}(v_2^2, [p_T])}{\sqrt{\text{Var}(v_2^2)_{dyn}} \sqrt{\text{Var}([p_T])_{dyn}}} \quad (1)$$

$\rho(c_2\{2\}, [p_T])$



Subevents A and B are used for calculation of $c_2\{2\}$; $|\eta| < 0.5$ for $[p_T]$

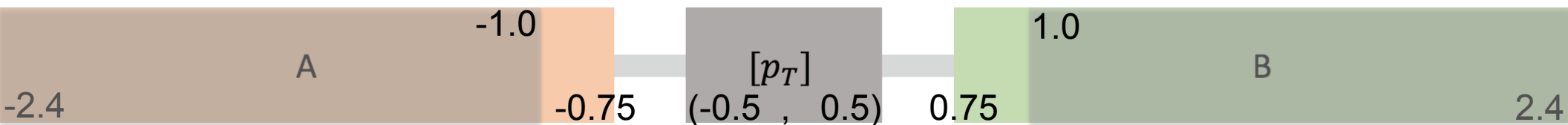


CMS Silicon Tracker, JINST 3 (2008) S08004

ANALYSIS METHOD (1)

$$\rho(v_2^2, [p_T]) = \frac{\text{cov}(v_2^2, [p_T])}{\sqrt{\text{Var}(v_2^2)_{dyn}} \sqrt{\text{Var}([p_T])_{dyn}}} \quad (1)$$

$\rho(c_2\{2\}, [p_T])$



Subevents A and B are used for calculation of $c_2\{2\}$; $|\eta| < 0.5$ for $[p_T]$

Covariance between $c_2\{2\}$ and $[p_T]$:

$$\text{cov}(c_2\{2\}, [p_T]) = \Re \left\langle \sum_{a,b} \exp^{2i(\phi_a - \phi_b)} ([p_T] - \langle [p_T] \rangle) \right\rangle \quad (2)$$

Dynamic variance of $c_2\{2\}$:

$$\text{Var}(c_2\{2\})_{dyn} = \langle \langle 4 \rangle \rangle - \langle \langle 2 \rangle \rangle^2 \quad (3)$$

Variance of $[p_T]$ from dynamic $[p_T]$ fluctuation c_k :

$$c_k = \left\langle \left[(p_{Ti} - \langle [p_T] \rangle) (p_{Tj} - \langle [p_T] \rangle) \right] \right\rangle \quad (4)$$

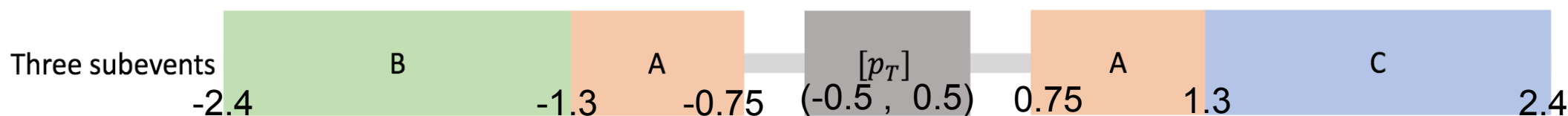
ANALYSIS METHOD (2)

$$\rho(v_2^2, [p_T]) = \frac{\text{cov}(v_2^2, [p_T])}{\sqrt{\text{Var}(v_2^2)_{dyn}} \sqrt{\text{Var}([p_T])_{dyn}}} \quad (1)$$



Extend and study the new variable to remove more nonflow

$$\rho(c_2\{2\}, [p_T]) \quad \longrightarrow \quad \rho(c_2\{4\}, [p_T])$$



$c_2\{4\}$ is analyzed with three subevent method

$$c_2\{4\}_{3\text{-sub}} = \langle 4 \rangle_{a,a|b,c} - 2\langle 2 \rangle_{a|b} \langle 2 \rangle_{a|c}$$

Phys. Rev. C 96, 034906 (2017)

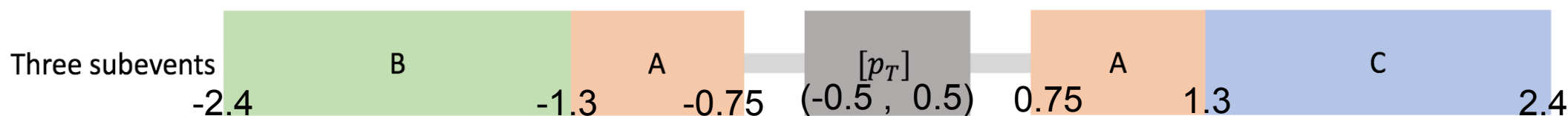
ANALYSIS METHOD (2)

$$\rho(v_2^2, [p_T]) = \frac{\text{COV}(v_2^2, [p_T])}{\sqrt{\text{Var}(v_2^2)_{dyn}} \sqrt{\text{Var}([p_T])_{dyn}}} \quad (1)$$



Extend and study the new variable to remove more nonflow

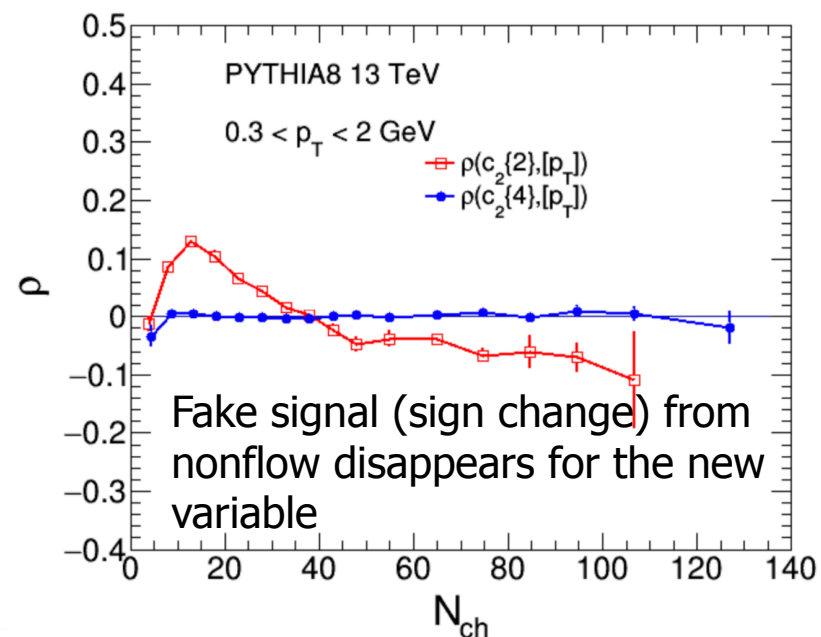
$$\rho(c_2\{2\}, [p_T]) \quad \longrightarrow \quad \rho(c_2\{4\}, [p_T])$$



$c_2\{4\}$ is analyzed with three subevent method

$$c_2\{4\}_{3\text{-sub}} = \langle 4 \rangle_{a,a|b,c} - 2\langle 2 \rangle_{a|b} \langle 2 \rangle_{a|c}$$

Phys. Rev. C 96, 034906 (2017)



Observables in this analysis

- This analysis focuses on small systems
- It is the first paper to :
 - use multiparticle correlations for flow when correlating with $[p_T]$
 - explore the correlator with different η gaps to study nonflow effects
 - measure $v_3 - [p_T]$ correlations in small systems
 - include measurements in pp collisions

Results

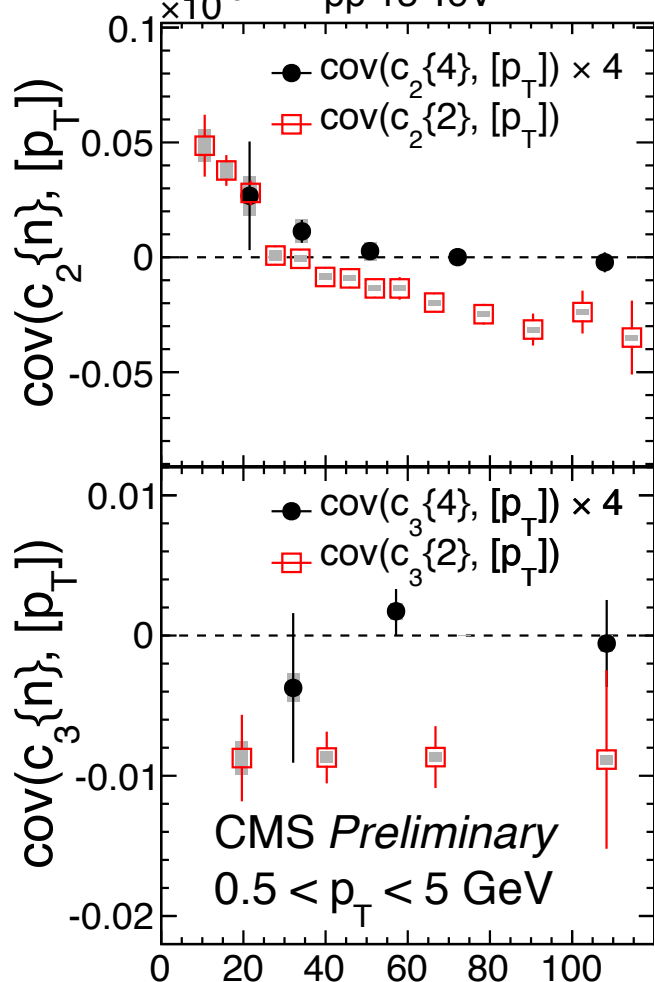
Results are presented as a function of N_{ch} , which is defined in $0.5 < p_T < 5.0$ GeV, $|\eta| < 2.4$, and corrected for tracking efficiency

RESULTS FOR COVARIANCE

CMS-PAS-HIN-21-012

pp 13 TeV

$n=2$

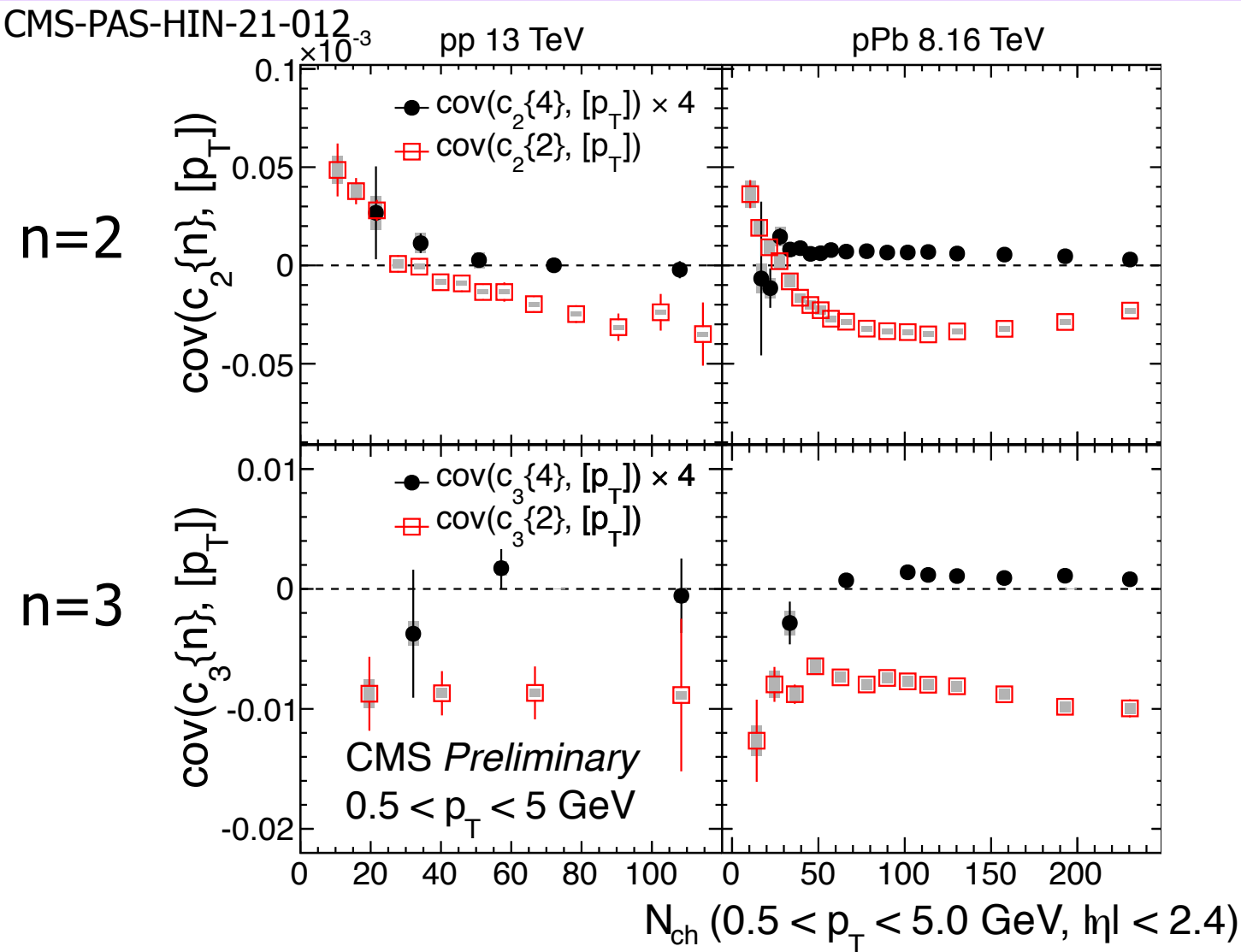


$N_{ch} (0.5 < p_T < 5.0 \text{ GeV}, |\eta| < 2.4)$



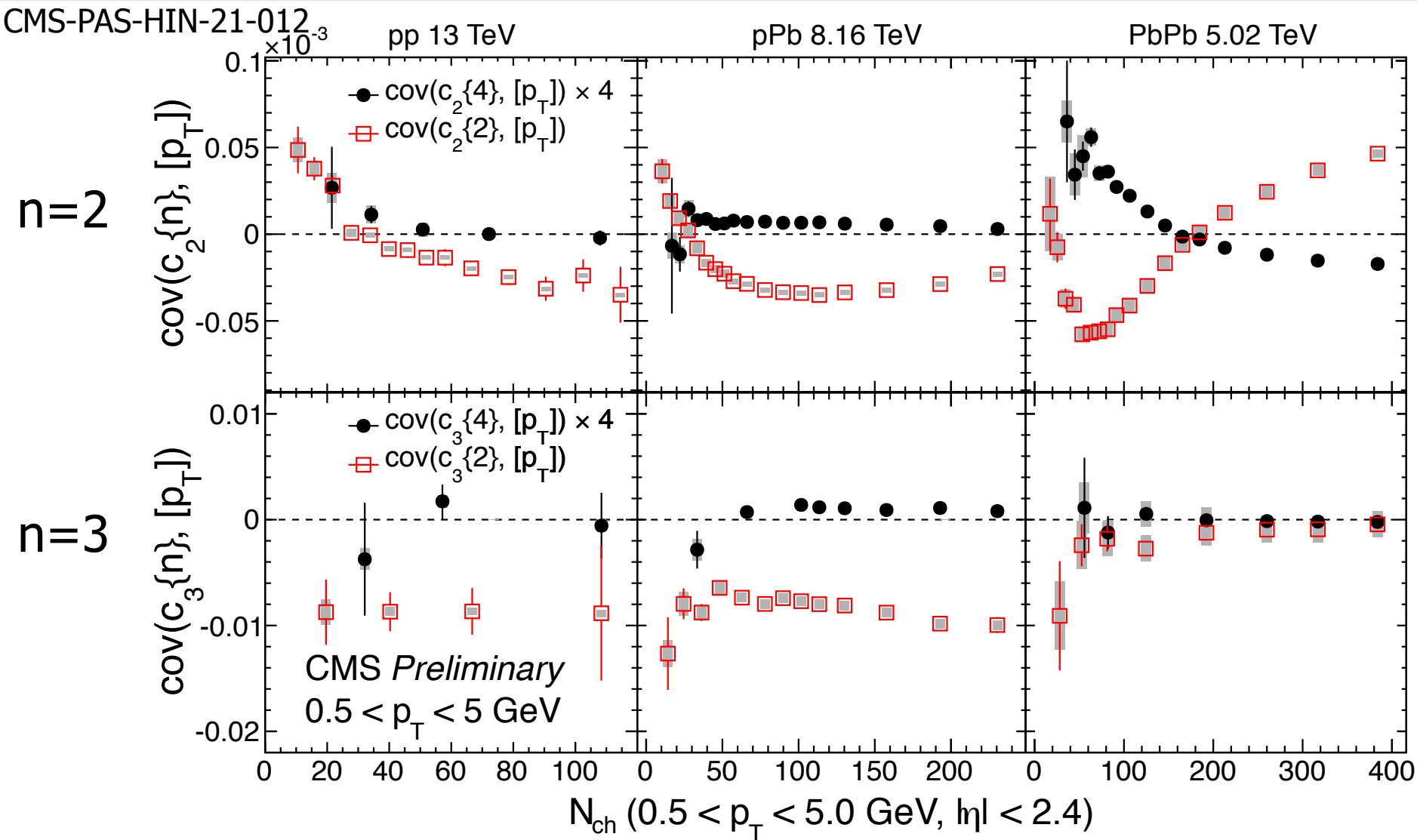
- Clear sign change for pp collisions with $c_2\{2\}$
- No sign change at low N_{ch} using multiparticle correlations with current statistics
- The sign of the normalized correlator is determined by the covariance

RESULTS FOR COVARIANCE



- Clear sign change for pp and pPb collisions with $c_2\{2\}$
- No sign change at low N_{ch} using multiparticle correlations with current statistics
- The sign of the normalized correlator is determined by the covariance

RESULTS FOR COVARIANCE



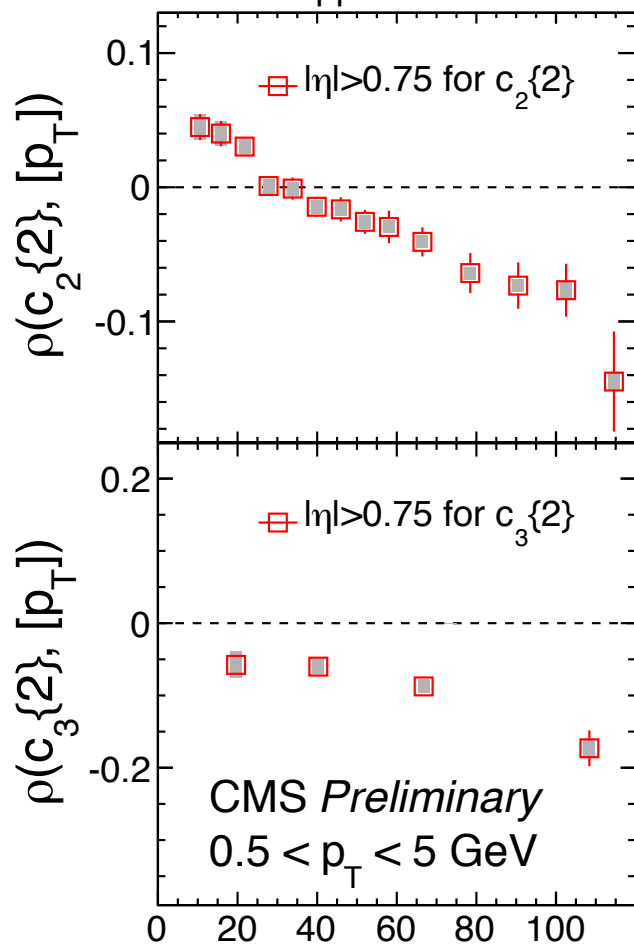
- Clear sign change for pp and pPb collisions with $c_2\{2\}$
- No sign change at low N_{ch} using multiparticle correlations with current statistics
- The sign of the normalized correlator is determined by the covariance

RESULTS FOR THE CORRELATOR

CMS-PAS-HIN-21-012

pp 13 TeV

$n=2$



$N_{ch} (0.5 < p_T < 5.0 \text{ GeV}, |\eta| < 2.4)$

-0.75
A

0.75
B



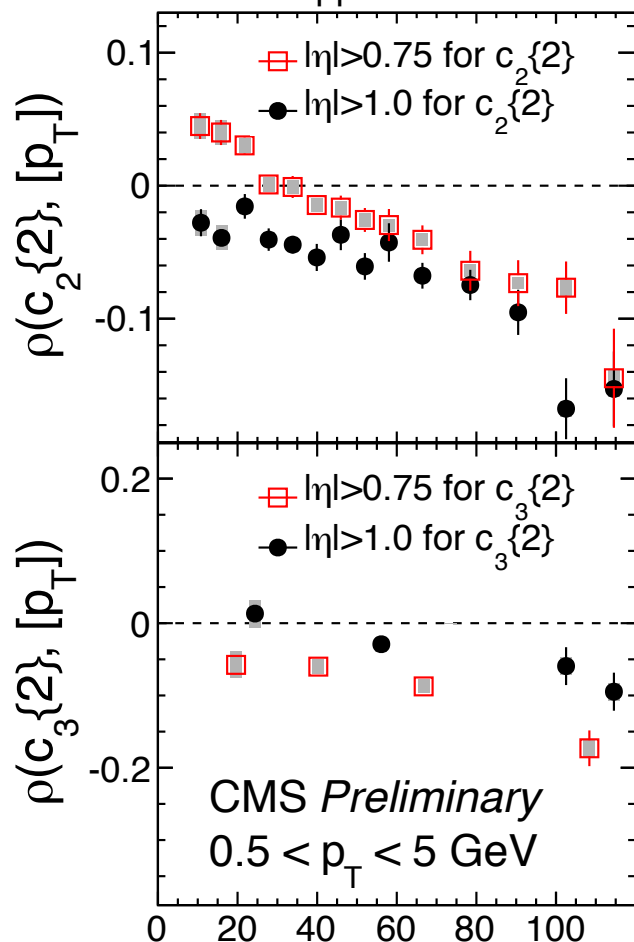
- Apparent sign change for $\rho(c_2^2, [p_T])$ in pp collisions

RESULTS FOR THE CORRELATOR

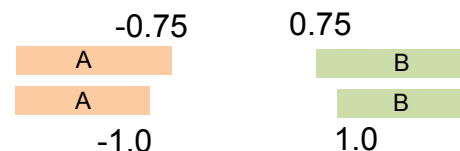
CMS-PAS-HIN-21-012

pp 13 TeV

$n=2$



$N_{ch} (0.5 < p_T < 5.0 \text{ GeV}, |\eta| < 2.4)$



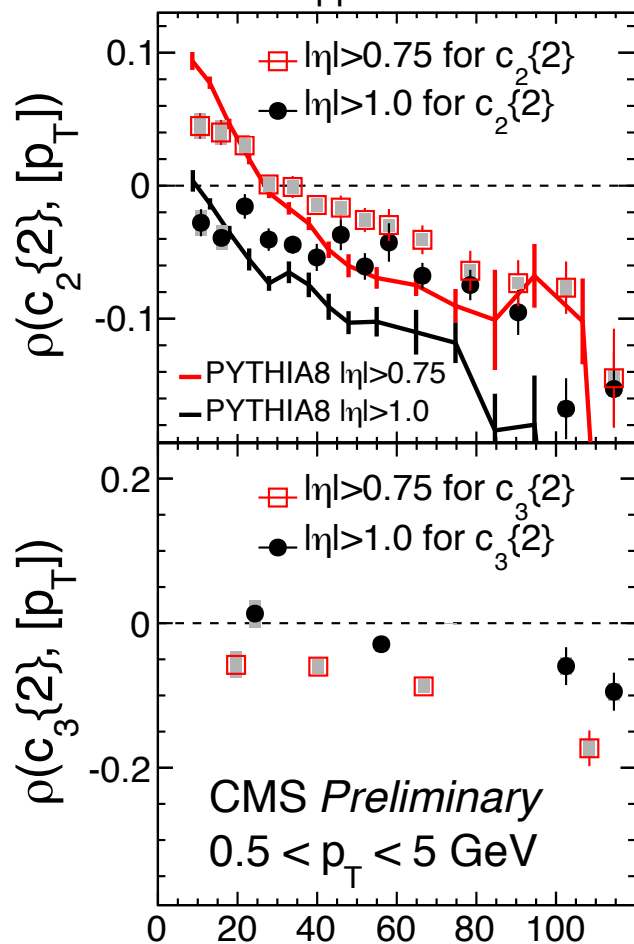
- Apparent sign change for $\rho(c_2^2, [p_T])$ in pp collisions
- However, no sign change is observed when using $|\eta| > 1.0$ for c_2^2

RESULTS FOR THE CORRELATOR

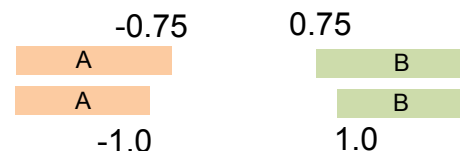
CMS-PAS-HIN-21-012

pp 13 TeV

$n=2$



$N_{ch} (0.5 < p_T < 5.0 \text{ GeV}, |\eta| < 2.4)$



- Apparent sign change for $\rho(c_2\{2\}, [p_T])$ in pp collisions
- However, no sign change is observed when using $|\eta| > 1.0$ for $c_2\{2\}$
- Also true for PYTHIA8 events

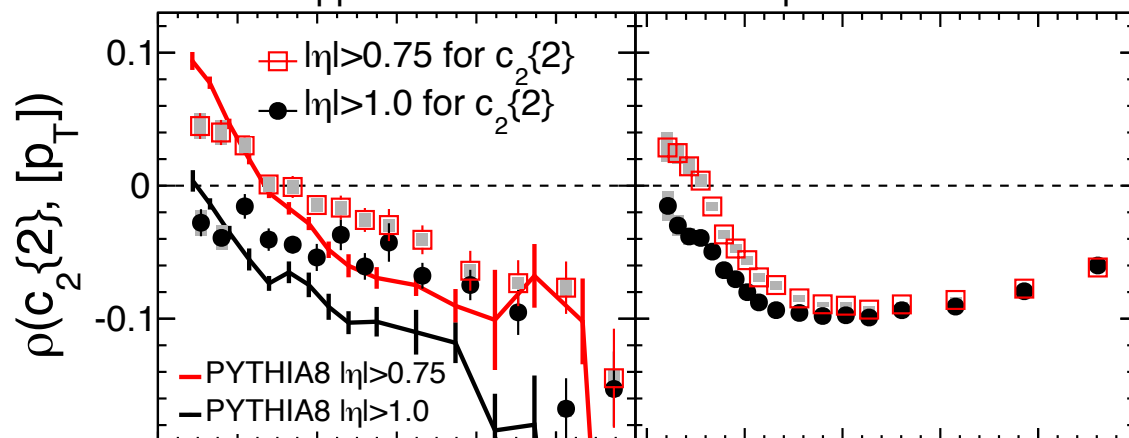
RESULTS FOR THE CORRELATOR

CMS-PAS-HIN-21-012

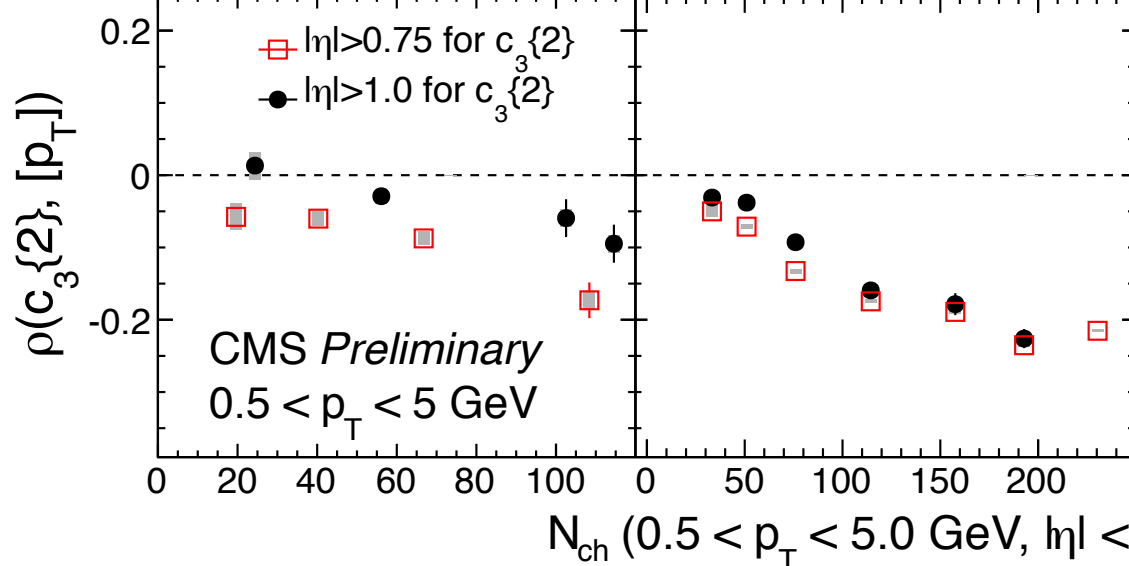
pp 13 TeV

pPb 8.16 TeV

$n=2$



$n=3$



- Apparent sign change for $\rho(c_2\{2\}, [p_T])$ in pPb \rightarrow agree with IP-Glasma+hydro
- However, no sign change is observed when using $|\eta| > 1.0$ for $c_2\{2\}$

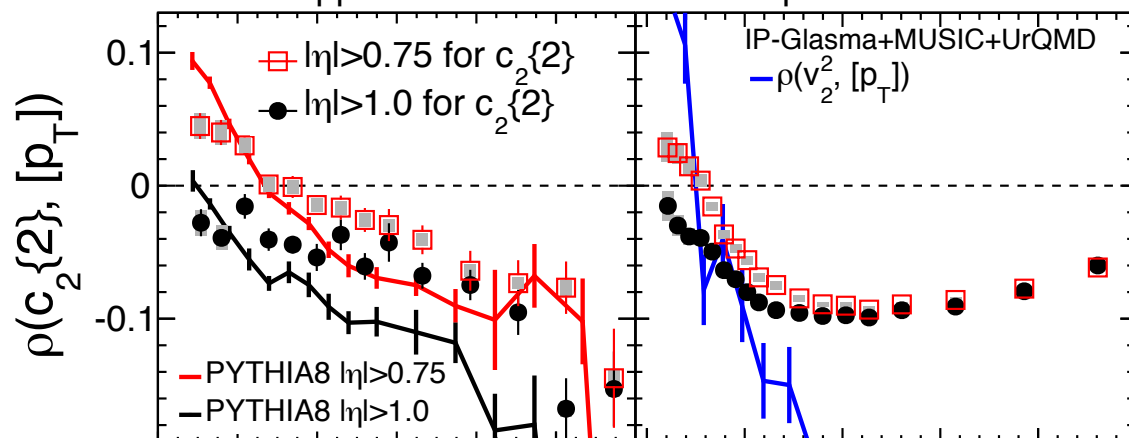
RESULTS FOR THE CORRELATOR

CMS-PAS-HIN-21-012

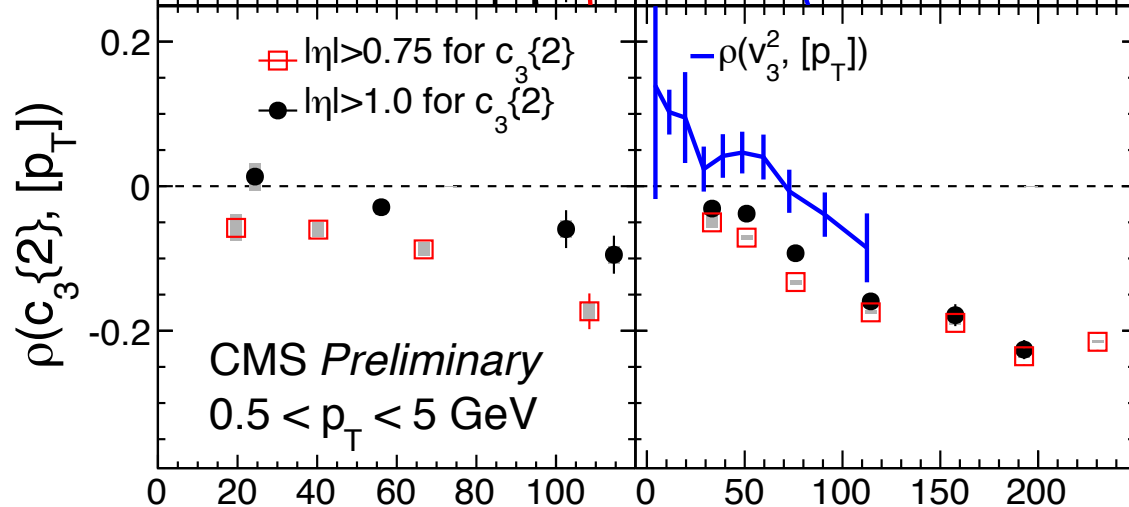
pp 13 TeV

pPb 8.16 TeV

$n=2$

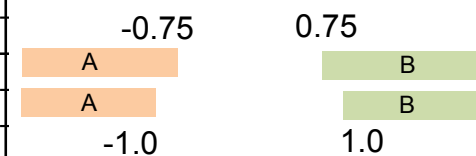


$n=3$



CMS Preliminary
 $0.5 < p_T < 5 \text{ GeV}$

$N_{ch} (0.5 < p_T < 5.0 \text{ GeV}, |\eta| < 2.4)$



- Apparent sign change for $\rho(c_2\{2\}, [p_T])$ in pPb -> agree with IP-Glasma+hydro
- However, no sign change is observed when using $|\eta| > 1.0$ for $c_2\{2\}$
- After removing nonflow with larger η gap, no evidence of CGC in data

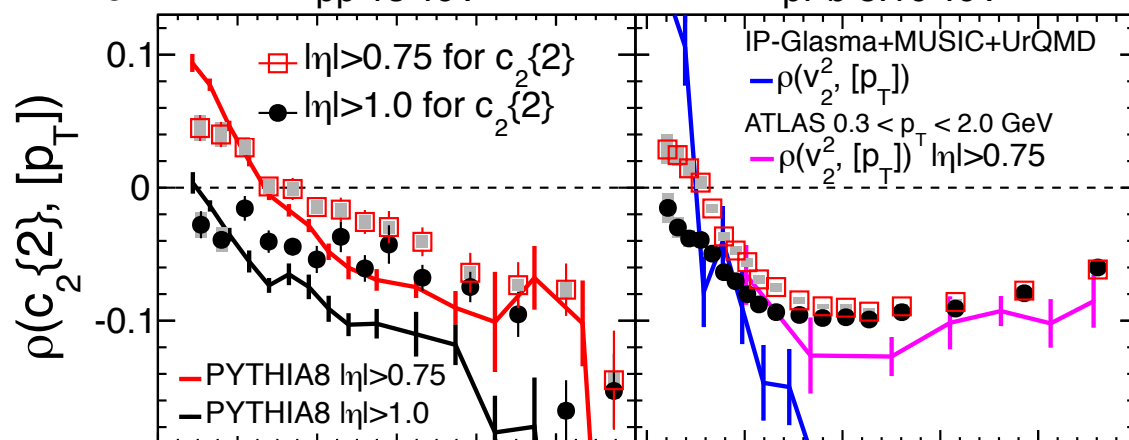
RESULTS FOR THE CORRELATOR

CMS-PAS-HIN-21-012

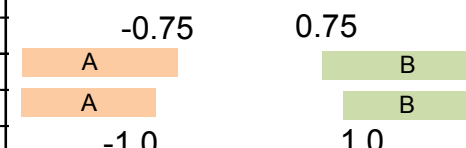
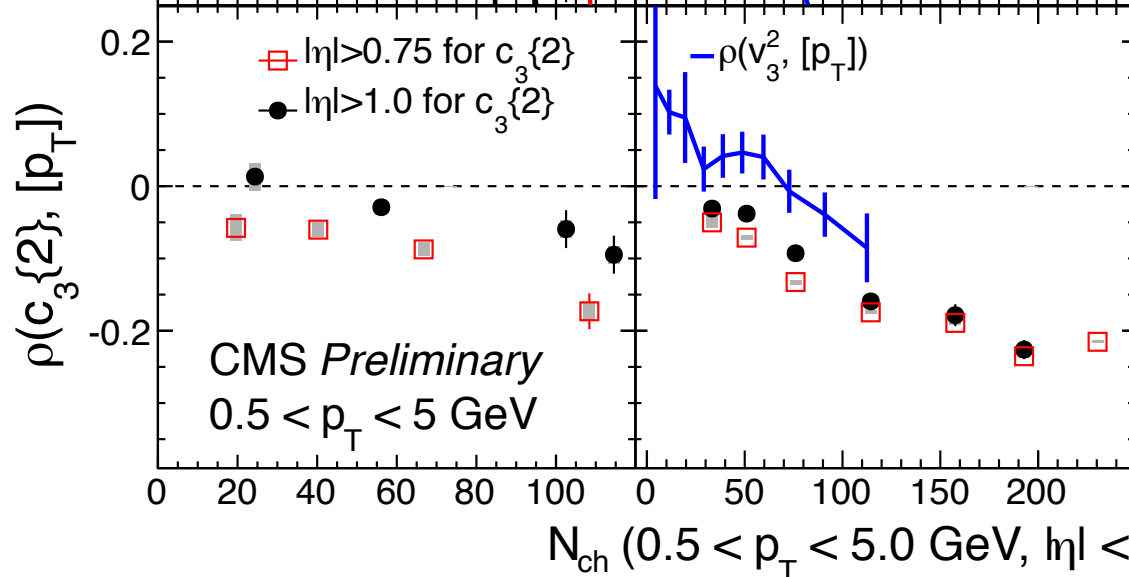
pp 13 TeV

pPb 8.16 TeV

$n=2$



$n=3$



- Apparent sign change for $\rho(c_2\{2\}, [p_T])$ in pPb -> agree with IP-Glasma+hydro
- However, no sign change is observed when using $|\eta| > 1.0$ for $c_2\{2\}$
- After removing nonflow with larger η gap, no evidence of CGC in data

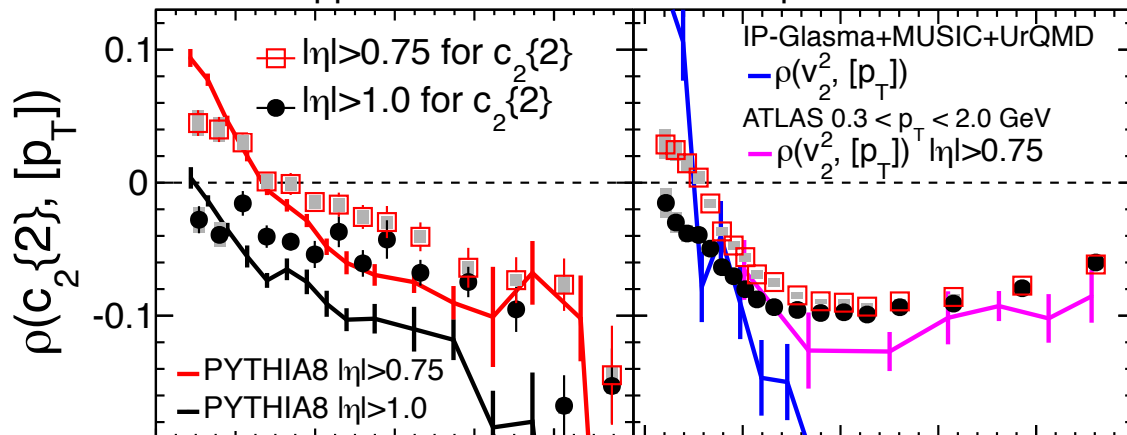
RESULTS FOR THE CORRELATOR

CMS-PAS-HIN-21-012

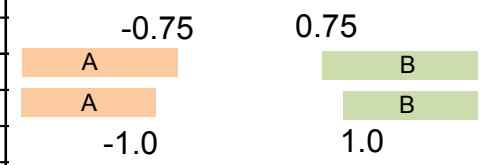
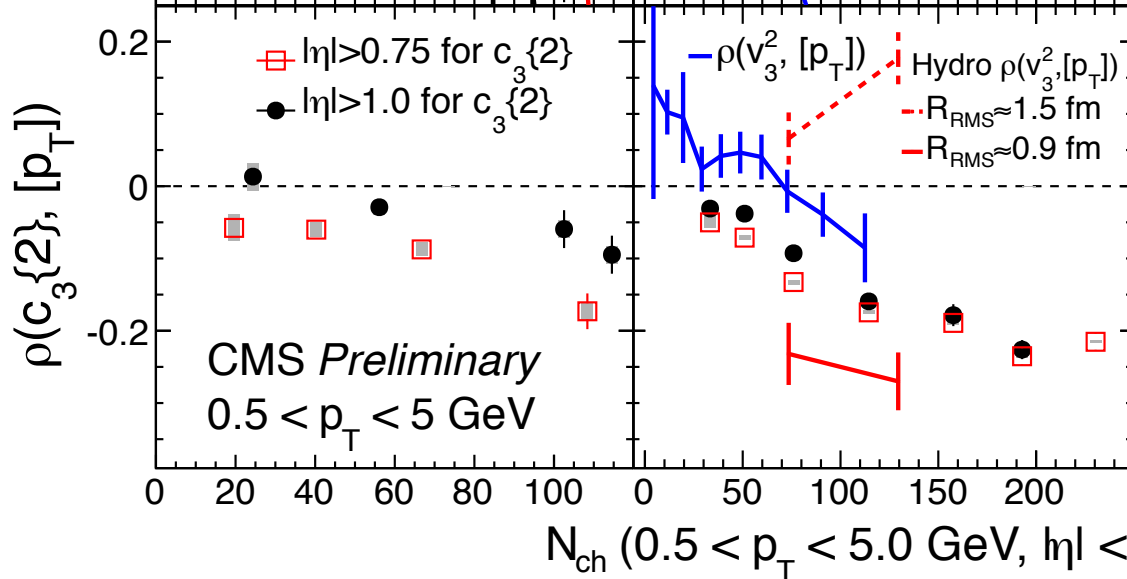
pp 13 TeV

pPb 8.16 TeV

$n=2$

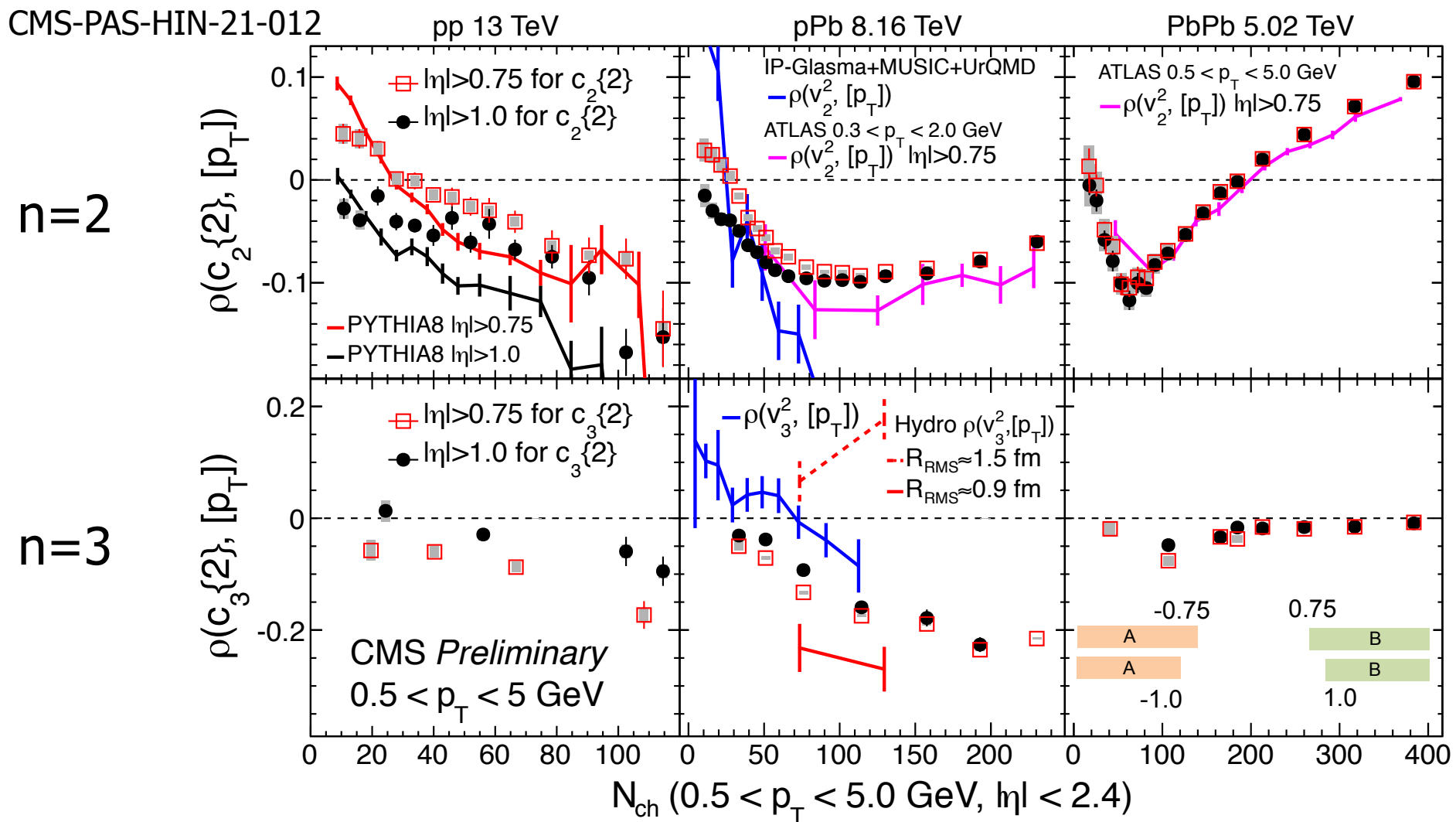


$n=3$



- Apparent sign change for $\rho(c_2\{2\}, [p_T])$ in pPb \rightarrow agree with IP-Glasma+hydro
- However, no sign change is observed when using $|\eta| > 1.0$ for $c_2\{2\}$
- After removing nonflow with larger η gap, no evidence of CGC in data
- Data better described by the smaller initial fireball $R_{\text{RMS}} = 0.9$ fm in hydro

RESULTS FOR THE CORRELATOR



- Apparent sign change for $\rho(c_2\{2\}, [p_T])$ in pPb -> agree with IP-Glasma+hydro
- However, no sign change is observed when using $|\eta| > 1.0$ for $c_2\{2\}$
- After removing nonflow with larger η gap, no evidence of CGC in data
- Data better described by the smaller initial fireball $R_{RMS} = 0.9 \text{ fm}$ in hydro

SUMMARY

- For the first time, the correlations between $[p_T]$ and cumulants from both two- and four-particle correlations in small systems are presented
- Apparent sign change is observed for $\rho(c_2\{2\}, [p_T])$ in pp and pPb
- However, no sign change is observed with larger η gap in $c_2\{2\}$
 - ATLAS default is $|\eta| > 0.75$, with $|\Delta\eta| > 1.5$
 - ALICE default is $|\eta| > 0.4$, with $|\Delta\eta| > 0.8$
 - CMS is studying both $|\eta| > 0.75$ ($|\Delta\eta| > 1.5$) and $|\eta| > 1.0$ ($|\Delta\eta| > 2.0$)
- After removing more nonflow with both two- and four-particle correlation cumulants, there is no evidence of CGC in data
- These high-precision data and the observables employing multiparticle correlations should provide new insight into the origin of azimuthal anisotropy in small collision systems

Backup

ANALYSIS METHOD (3)

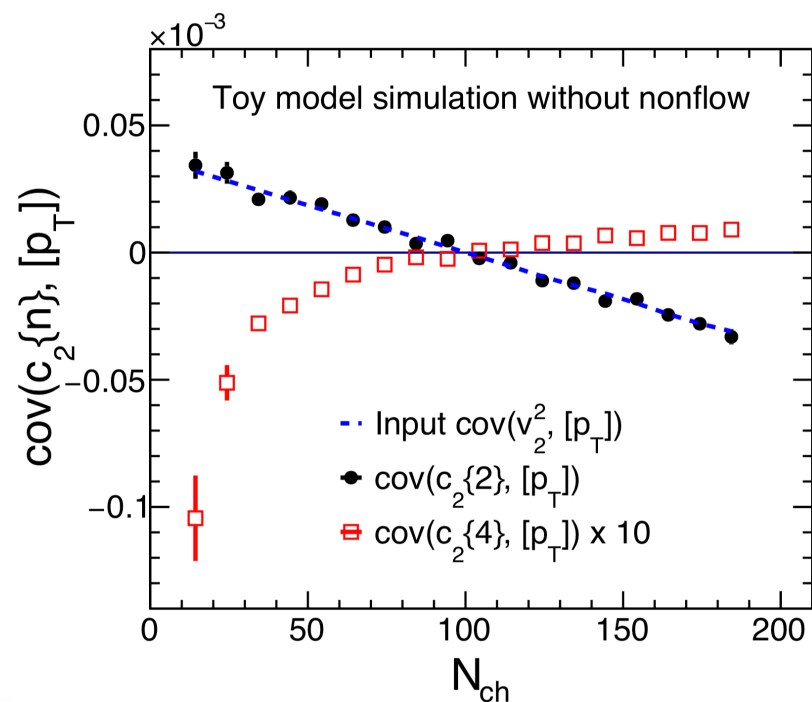
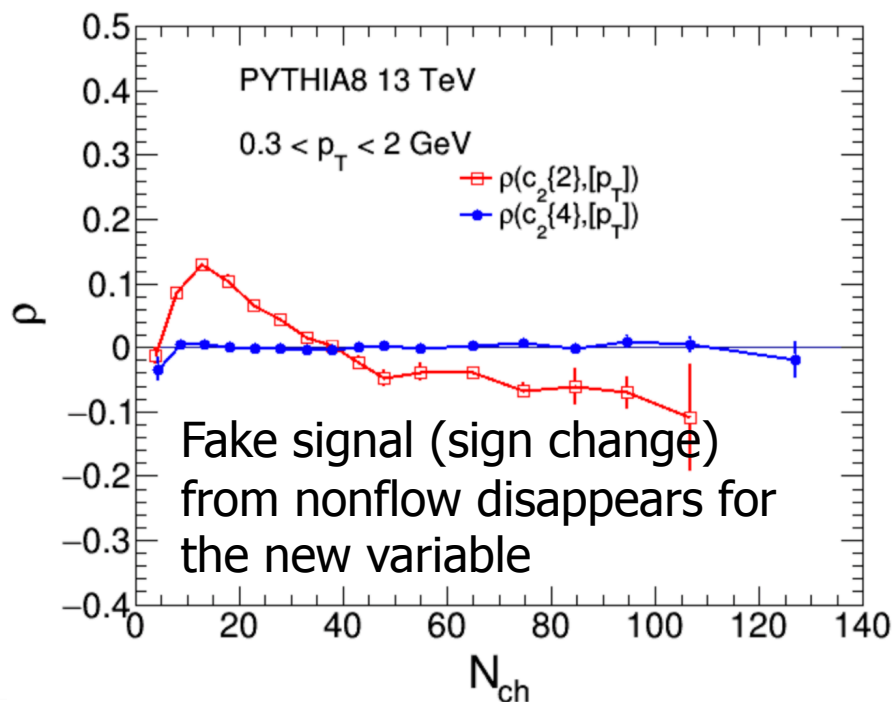
$$\rho(v_2^2, [p_T]) = \frac{\text{cov}(v_2^2, [p_T])}{\sqrt{\text{Var}(v_2^2)}\sqrt{\text{Var}([p_T])}} \quad (1)$$



Extend and study the new variable to remove more nonflow

$$\rho(c_2\{2\}, [p_T]) \quad \longrightarrow \quad \rho(c_2\{4\}, [p_T])$$

$c_2\{4\}$ is analyzed with three subevent method

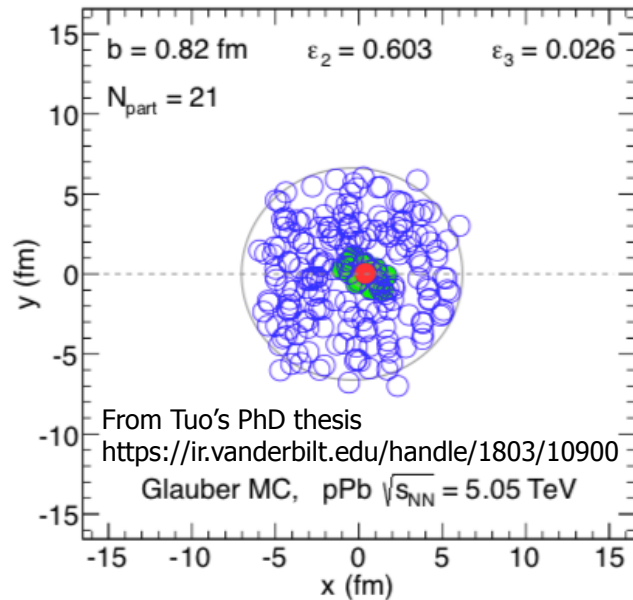


DYNAMIC FLOW FLUCTUATIONS

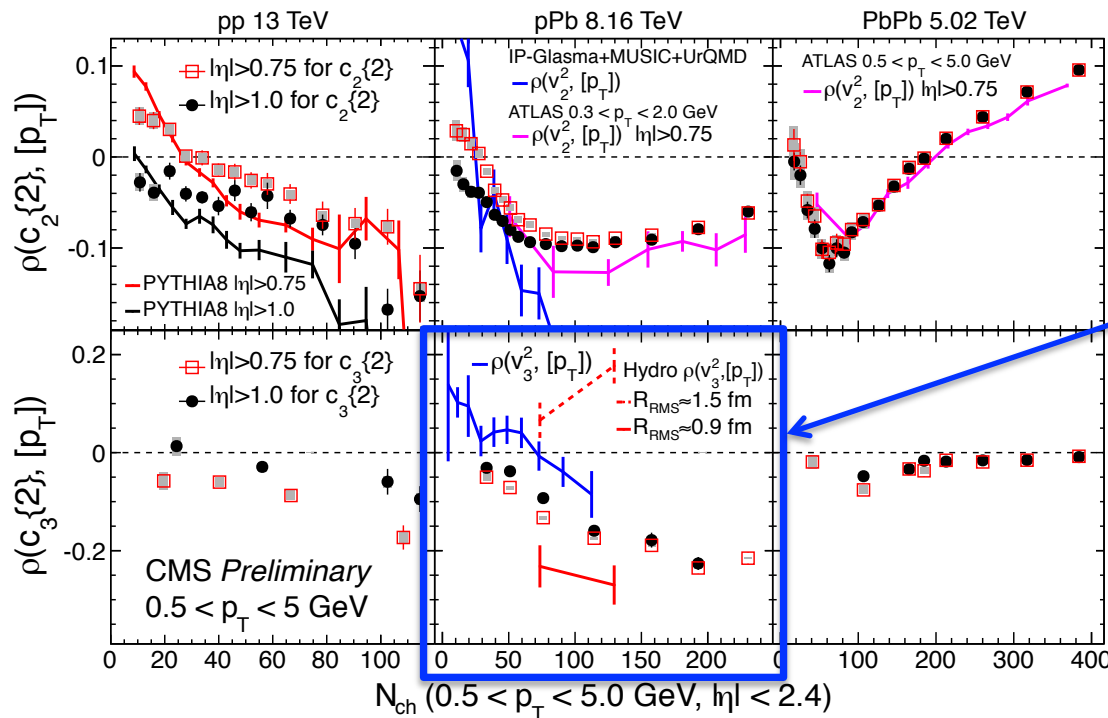
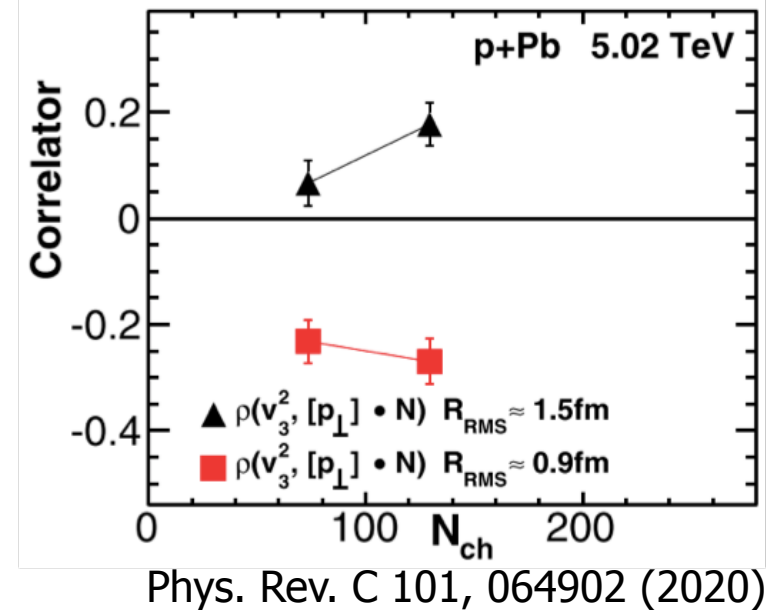
Keeping $\text{cov}(c_2\{4\}, [p_T])$ but drop $\rho(c_2\{4\}, [p_T])$ in this analysis

- The reason is we are not 100% sure if the variance $\text{Var}(c_2\{4\})_{\text{dyn}}$ in our new method is truly dynamic
- It may contain statistical fluctuations in our current method
- The measurement of v_n fluctuation in small systems is a task our community has not accomplished. The event-by-event v_n studies all stopped at 60-70% centrality in AA collisions

HYDRODYNAMIC PREDICTION IN PPB FOR N=3



Average transverse size of the fireball in pPb collisions:
Is it close to $R_{\text{RMS}} = 1.5 \text{ fm}$ or 0.9 fm ?



• The data are qualitatively better described by the smaller initial fireball

MAPPING BETWEEN N_{CH} AND $N_{\text{TRK}}^{\text{OFFLINE}}$

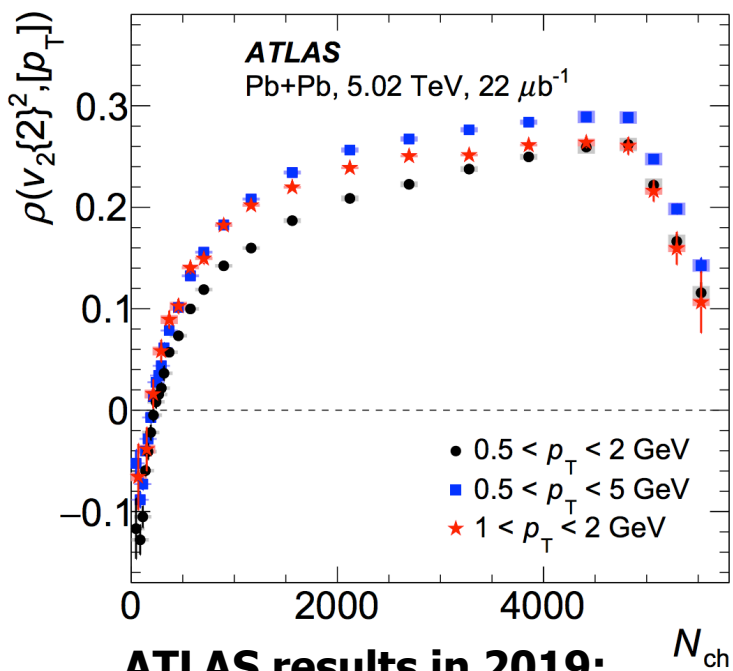
Table 1: Average multiplicity of reconstructed tracks per $N_{\text{ch}}^{\text{rec}}$ bin for N_{ch} and $N_{\text{trk}}^{\text{offline}}$ in pp, pPb, and PbPb collisions. Uncertainties for the tracking efficiency corrected N_{ch} are included.

$N_{\text{ch}}^{\text{rec}}$ range	pp		pPb		PbPb	
	$\langle N_{\text{ch}} \rangle$	$\langle N_{\text{trk}}^{\text{offline}} \rangle$	$\langle N_{\text{ch}} \rangle$	$\langle N_{\text{trk}}^{\text{offline}} \rangle$	$\langle N_{\text{ch}} \rangle$	$\langle N_{\text{trk}}^{\text{offline}} \rangle$
[0, 20)	8 ± 0.3	9	11 ± 0.4	12	16 ± 0.6	14
[20, 40)	34 ± 1	34	36 ± 1	36	57 ± 2	48
[40, 60)	58 ± 2	56	60 ± 2	60	96 ± 4	80
[60, 80)	82 ± 3	78	83 ± 3	82	135 ± 5	112
[80, 100)	106 ± 4	101	107 ± 4	105	175 ± 7	144
[100, 150)	132 ± 5	125	140 ± 6	137	240 ± 10	197
[150, 200)			198 ± 8	191	335 ± 13	276
[200, 250)			256 ± 10	246	434 ± 17	353
[250, 300)					535 ± 21	426

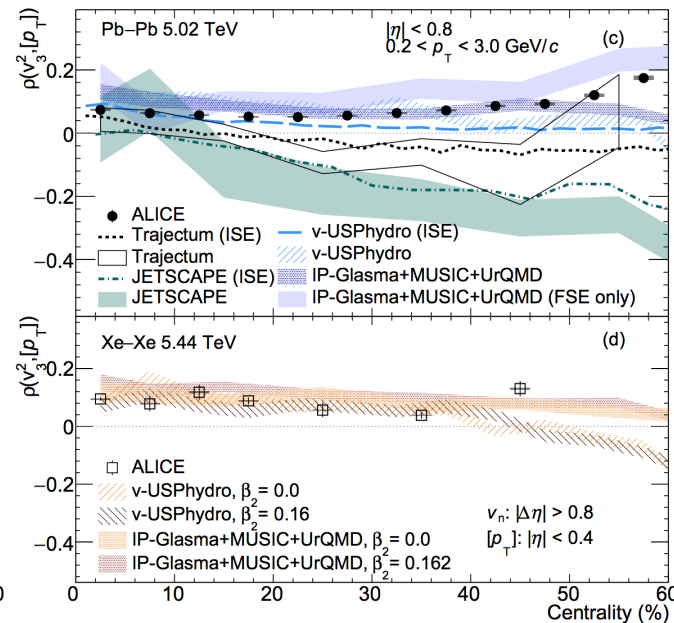
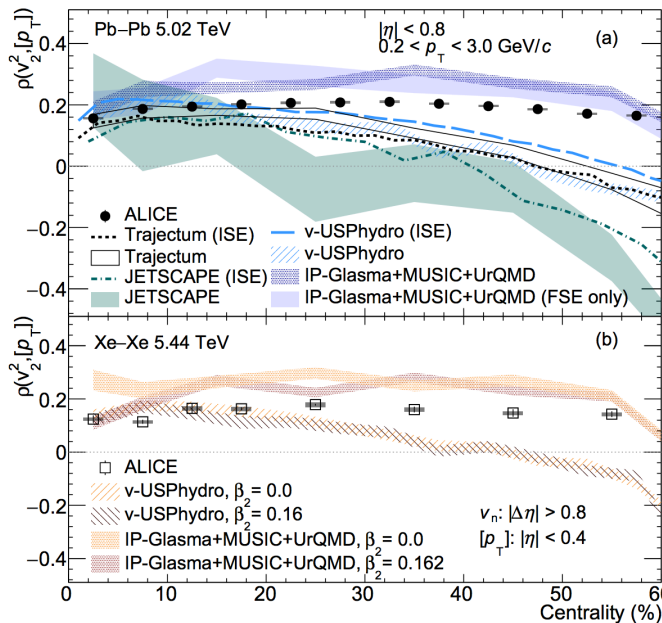
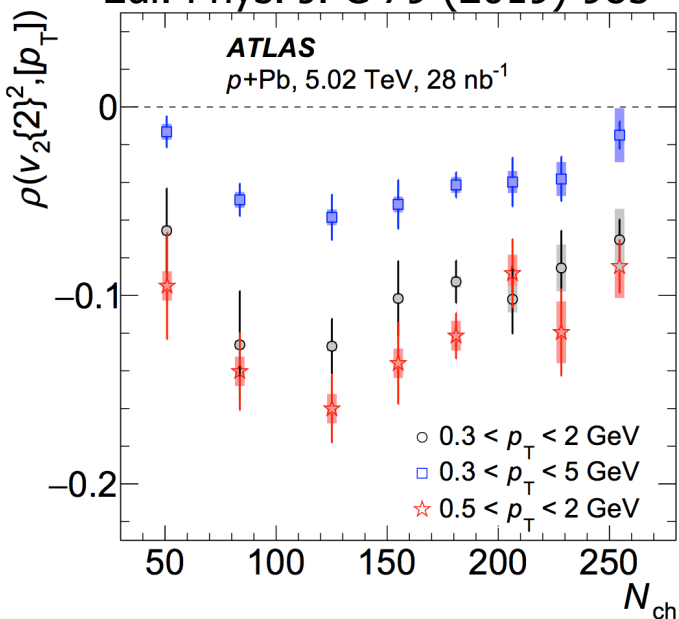
- The mapping table between N_{ch} and $N_{\text{trk}}^{\text{offline}}$

EXISTING MEASUREMENTS

ALICE: arXiv:2111.06106 submitted to PRL



ATLAS results in 2019:
Eur. Phys. J. C 79 (2019) 985



- ATLAS results in pPb, PbPb, and XeXe collisions
- ALICE results in PbPb and XeXe collisions
- Some recent studies from STAR

